DOI: 10.1002/ejic.201000321

Synthesis of AuNi/NiO Nanocables by Porous AAO Template Assisted Galvanic Deposition and Subsequent Oxidation

Qiaoling Xu,*[a] Guowen Meng,*[a] Bensong Chen,[a] Xiangdong Li,[a] Xiaoguang Zhu,[a] Zhaoqin Chu,[a] and Mingguang Kong[a]

Keywords: Nanocables / Nanostructures / Redox chemistry / Template synthesis

A facile and economic approach has been developed for the synthesis of coaxial nanocables with AuNi alloy nanowires as inner solid cores and NiO as outer shells by infiltrating a gold-coated anodic aluminum oxide (AAO) template, with ring-shaped Al foil on its outer edge, with a mixed aqueous solution of $NiCl_2$ and $HAuCl_4$ to form AuNi/Ni nanocables, and subsequent immersion in an aqueous NaOH solution to oxidize the Ni sheath during template removal. The formation of the AuNi/Ni nanocables in the channels of the AAO template could be ascribed to the reduction of the Ni^{2+} ion complexes adhering on the AAO channel walls and the redox reactions of two galvanic cells in which the surrounding Al foil acts as the anode. The approach enables excellent control over the shell thickness and the chemical composition of the AuNi/NiO nanocable by tuning the composition of the mixed solution. The AuNi/NiO nanocables have potentials in nanodevices and nanosystems.

Introduction

One-dimensional hybrid nanoarchitectures, especially coaxial nanocables consisting of a core/shell heterojunction in the radial direction, have great potential in nanotechnological applications, such as in sensors,[1,2] transistors,[3,4] solar cells,[5] and power sources.[6] To date, various approaches have been developed for nanocables, such as electrochemical deposition to prepare metal/metal, metal/semimetal, and metal/oxide nanocables;[7–9] sol–gel methods for metal/silica nanocables,[10,11] hydrothermal routes to Ag/C nanocables;[12,13] in situ oxidation reactions for Ag/AgCl nanocables;[14] vapor-liquid-solid processes to obtain metal/semiconductor[15,16] and semiconductor/insulator nanocables,[1,17] and self-assembly processes for Au/polymer nanocables.[18,19] However, in the above-mentioned methods, either electric power or capping agents are used, or high-temperature reactions are involved. Therefore, exploiting low-cost and convenient synthetic approaches to nanocables still remains a challenge.

In our previous work,[20] we developed a facile, economic, and generic way to mono- and multisegment metallic nanowires (NWs) of various pure metals and their alloys with both linear and branched topologies, by merely infiltrating Au-coated native porous anodic aluminum oxide (AAO) templates with ring-shaped Al foil on their outer edge (to be abbreviated as "Au-coated-Al-surrounded AAO templates") with aqueous solutions of metal chloride salts. As Ni^{2+} ions form chemical complexes with hydroxy groups on the AAO channel walls,[7] if a mixed aqueous solution containing Ni^{2+} ions is employed, Ni^{2+} ions would be absorbed on the channel walls of the AAO template, and nanocables with Ni-related materials as outer shells could be formed by such an approach. Here, by infiltrating the Au-coated-Al-surrounded AAO template with a mixed aqueous solution of $NiCl_2$ and $HAuCl_4$, followed by immersing the as-infiltrated AAO template in an aqueous NaOH solution, nanocables with AuNi alloy NWs as inner solid cores and nickel monoxide (NiO) as outer sheaths (to be abbreviated as "AuNi/NiO nanocables") have been obtained.

Results and Discussion

The infiltration was carried out in our previous set-up by using a mixed aqueous solution of $NiCl_2$ and $HAuCl_4$ rather than aqueous solutions of one kind of metal chloride salt or two metal chloride salts (not including $NiCl_2$) previously used for metallic and alloy NWs.[20] Subsequent immersion of the above as-infiltrated AAO template in an aqueous NaOH solution results in cable-like structures, as shown in Figure 1a. The nanocables have uniform diameters of 70–90 nm, in agreement with those of the nanochannels inside the AAO template. The enlarged transmission electron microscopy (TEM, JEM-2010) image of a single nanocable (inset of Figure 1a) clearly displays the

[a] Key Laboratory of Materials Physics, and Anhui Key Laboratory of Nanomaterials and Nanostructures, Institute of Solid State Physics, Chinese Academy of Sciences,
Hefei, Anhui 230031, P. R. China
Fax: +86-551-5591434
E-mail: qlxu@issp.ac.cn
gwmeng@issp.ac.cn

Supporting information for this article is available on the WWW under http://dx.doi.org/10.1002/ejic.201000321.

 © 2010 Wiley-VCH Verlag GmbH & Co. KGaA, Weinheim View this journal online at wileyonlinelibrary.com

interfaces between the inner core and the outer shell of the nanocable. A lattice-resolved TEM image of the core–shell interface of the nanocable (Figure 1b) reveals that the inner solid core and the outer shell are composed of AuNi alloy and NiO, respectively. Energy-dispersive X-ray (EDX) elemental line-scanning data (Figure 1c) and mapping (Figure 1d) exhibit that the elements O and Ni are present across the whole nanocable, while elemental Au is only present in the inner core part, further demonstrating the AuNi-core/NiO-shell structure of the nanocable. The EDX measurement (Figure 1e) also confirms that the nanocable is composed of Au, Ni, and O.

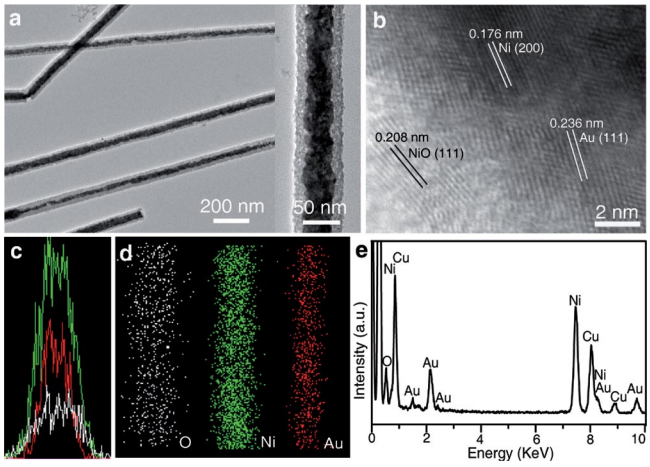

Figure 1. AuNi/NiO nanocables obtained by using a mixed aqueous solution with 2.4 M $NiCl_2$. (a) TEM image of the nanocables, the inset is an enlarged image of a single nanocable. (b) Lattice-resolved image of the core–shell interface of the nanocable. (c) EDX elemental line-scanning cross the nanocable shown in the inset of (a) (white for O, green for Ni, and red for Au). (d) EDX elemental mappings of O, Ni, and Au. (e) EDX spectrum taken from the nanocable shown in the inset of (a), where the Cu peaks are from the TEM grid.

To understand the influence of the composition of the mixed solution on the formation of the nanocables, different compositions were employed. Figure 2 shows the morphological evolution of the AuNi/NiO nanocables in mixed solutions with different $NiCl_2$ concentrations. From the enlarged images (insets of Figures 2a–c), the shell thickness (denoted as T_{shell}) and the core diameter (denoted as D_{core}) of the nanocables can be measured, and a shell-thickness/core-diameter ratio (T_{shell}/D_{core}) has been defined, as shown in Table 1. When the mixed solution with 2.4 M $NiCl_2$ is used, T_{shell}/D_{core} of the nanocable (Figure 2a) is about 0.53. When the concentration of $NiCl_2$ is reduced to 2 M, the T_{shell}/D_{core} decreases to about 0.2, indicating that the nanocable has a thinner shell (Figure 2b). At a much lower $NiCl_2$ concentration (1.6 M), the resultant nanocable (Figure 2c) has a much smaller T_{shell}/D_{core} value of about 0.11. Taken together, the NiO outer shell thickness of the nanocables decreases with the reduction of the $NiCl_2$ concentration in the mixed solution. EDX analyses have been performed to investigate the detailed chemical composition of the nanocables. The analysis results for the three kinds of nanocables were obtained by measuring four arbitrary points along each nanocable. We defined the ratio of the atomic percentages of Ni to Au as "Ni/Au%" and calculated its average value from the four groups of data measured. From the calculated Ni/Au% for the three kinds of nanocables (shown in Table 1), it can be concluded that the lower the molar concentration of the $NiCl_2$ in the mixed solution is, the smaller the Ni/Au% the nanocable has. Thus, by controlling the composition of the mixed solutions, the NiO outer shell thickness and the chemical composition of the AuNi/NiO nanocables can be tuned at will.

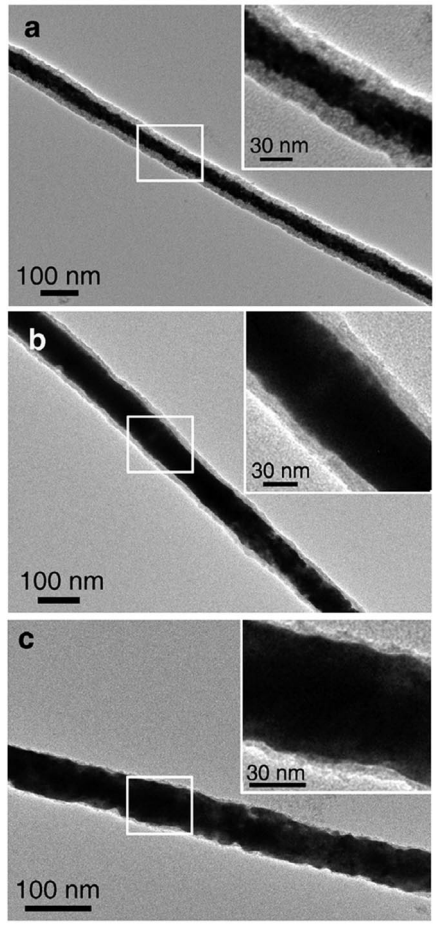

Figure 2. TEM images of the AuNi/NiO nanocables prepared in mixed solutions with different $NiCl_2$ concentrations of (a) 2.4 M, (b) 2 M, and (c) 1.6 M. The insets are the enlarged images of the nanocables taken from the areas marked with white rectangles.

Table 1. T_{shell}, D_{core}, T_{shell}/D_{core} and Ni/Au% of the three kinds of nanocables.

Sample[a]	T_{shell} (nm)	D_{core} (nm)	T_{shell}/D_{core}	Ni/Au (%)
I	16.00	30.00	0.53	3.62
II	12.90	64.65	0.20	1.89
III	6.45	61.30	0.11	0.39

[a] Samples I, II, and III are the nanocables shown in Figures 2a, b, and c, respectively.

 © 2010 Wiley-VCH Verlag GmbH & Co. KGaA, Weinheim

X-ray diffraction (XRD) measurements have been performed on the as-infiltrated AAO templates obtained in mixed solutions with different $NiCl_2$ concentrations before being immersed in aqueous NaOH solutions, as shown in Figure S1. For the samples obtained in the mixed solution with 2.4 M $NiCl_2$, the XRD spectrum (Figure S1a) shows the peaks of face-centered cubic (fcc) Ni without any peaks related to pure Au. When the $NiCl_2$ concentrations in the mixed solutions are decreased to 2 or 1.6 M, XRD spectra of the resultant products (Figures S1b or c, respectively) only exhibit the peaks of fcc Au. Combining these phenomena with the results shown above, it can be deduced that a high concentration of $NiCl_2$ in the mixed solution may lead to Ni-rich AuNi solid solutions in the nanochannels of the AAO template, whereas a lower concentration of $NiCl_2$ may result in Au-rich AuNi solid solutions in the nanochannels of the AAO template.

On the basis of the above results and the formation mechanism of metallic NWs in our previous work,[20] we now propose a possible formation mechanism for the AuNi/NiO nanocables, as shown in Figure 3a schematically. It is well known that certain metal/metal–ion pairs are spontaneously oxidized and reduced in solution. For example, when Zn [Zn^{3+}/Zn, –0.7626 V vs. SHE (standard hydrogen electrode)] is exposed to a Cu^{2+} (Cu^{2+}/Cu, +0.34 V vs. SHE) solution,[21] spontaneous oxidation of Zn to Zn^{2+} and reduction of Cu^{2+} to Cu occur, leading to a familiar galvanic cell. In our experiments, once the mixed solution of $NiCl_2$ and $HAuCl_4$ reaches the ring-shaped Al foil outside the porous AAO, chloride ions in the solution etch away the dull alumina layer on the pure Al foil.[22] Thus, pure Al is exposed to the mixed solution, leading to galvanic cells on its surface due to the lower redox potential of pure Al [Al^{3+}/Al, –1.67 V vs. SHE] than those of Ni^{2+} (Ni^{2+}/Ni, –0.257 V vs. SHE) and $AuCl_4^-$ ions ($AuCl_4^-$/ Au, + 1.002 V vs. SHE).[21] In these galvanic cells (the top one), some locations on the Al foil surface serve as the anode and some other locations act as the cathode. At the anode, Al is oxidized to Al^{3+}, which subsequently enters into the solution [Equation (1)].

$$Al \rightarrow Al^{3+} + 3e^- \quad (1)$$

At the cathode, $AuCl_4^-$ and Ni^{2+} ions are reduced to Au and Ni atoms [Equations (2) and (3)], respectively.

$$AuCl_4^- + 3e^- \rightarrow Au + 4Cl^- \quad (2)$$

$$Ni^{2+} + 2e^- \rightarrow Ni \quad (3)$$

As the radii of Au^{3+} and Cl^- are 0.85×10^{-10} and 1.81×10^{-10} m, respectively, the radius of the $AuCl_4^-$ ion, which is assumed to be the sum of the Au^{3+} and Cl^- radii, is 2.66×10^{-10} m. The radius of the Ni^{2+} ion is 0.69×10^{-10} m. The pore radii of the AAO templates are in the range 3.5–4.5 $\times 10^{-8}$ m, which is two orders of magnitude larger than the radii of the $AuCl_4^-$ and Ni^{2+} ions. It has been reported that the ratio of the diffusion coefficient for a molecule in the nanotube (D_{tube}) to its value in free solution (D_{sol}) is related to the ratio of the radius of the diffusing molecule (r_{mol}) to the radius of the nanotube (r_{tube}). For the extreme of $r_{mol} << r_{tube}$, $D_{tube}/D_{sol} = 1$.[23] In our case, the radii of the ions are much smaller than those of the pores of the AAO templates. Thus, the diffusion coefficient for the ions in the nanochannels is almost equivalent to that in solution, indicating good diffusivity for the ions in the nanochannels. When the nanochannels are infiltrated with the mixed solution containing $AuCl_4^-$ and Ni^{2+} ions and these ions reach the Au layer at the bottom of the nanochannels, another galvanic cell (the bottom one) is immediately formed, with the Al foil as anode and the Au layer (in good electrical contact with the Al foil) as cathode. Chemical reactions at the anode and the cathode are the same as those of the top galvanic cell shown in Equations (1)–(3).

Figure 3b shows different representative stages for the formation of the AuNi/NiO nanocables. At the initial stage of the infiltration process, both Au and Ni atoms are formed simultaneously on the ring-shaped Al foil by redox reactions at the top galvanic cell. When the nanochannels of the AAO template are further infiltrated with the mixed solution, chemical complexation of some Ni^{2+} ions with hydroxy groups on the AAO channel walls occurs,[7] and Ni^{2+} ion complexes containing two coordinate bonds may be

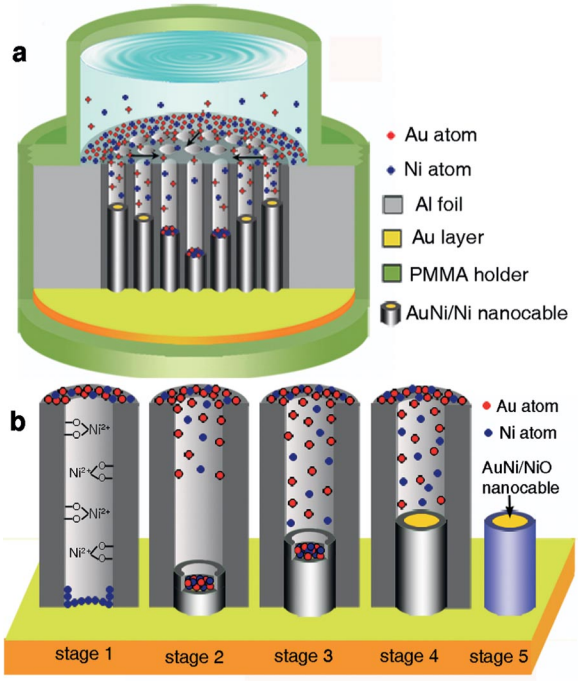

Figure 3. Schematics showing (a) the simple set-up for the infiltration process and (b) the formation process of the AuNi/NiO nanocables with five different representative stages: stage 1, the formation of Au and Ni atoms on the ring-shaped Al foil top surface and Ni nuclei around the bottom channel wall; stage 2, the formation of the AuNi/Ni nanocables with longer cable shells than cores and diffusion of the Au and Ni atoms from the Al foil surface into the nanochannel; stage 3, continuous growth of the Ni sheath and the growth of AuNi alloy NW from Au and Ni atoms coming from both the top and the bottom galvanic cells; stage 4, the formation of AuNi/Ni nanocables with the AuNi alloy cores almost as long as the Ni sheaths in the nanochannel; stage 5, the formation of AuNi/NiO nanocables during the removal of the AAO template in an aqueous NaOH solution.

 © 2010 Wiley-VCH Verlag GmbH & Co. KGaA, Weinheim

formed as a result of the combination of one Ni^{2+} ion with oxygen atoms of two hydroxy groups on the channel wall. As Ni^{2+} ions have a smaller volume than $AuCl_4^-$ ions, they reach the bottom of the nanochannels first, and most of them preferentially form Ni^{2+} ion complexes on the bottom channel walls. The Ni^{2+} ion complexes are then reduced to Ni atoms by redox reaction at the bottom galvanic cell, and Ni nuclei are formed around the bottom channel walls (Figure 3b, stage 1). With continuous reduction of Ni^{2+} ion complexes on the channel walls at the bottom galvanic cell, Ni nuclei grow upwards along the nanochannel walls to form the Ni nanotube as a cable shell. In addition to the formation of Ni^{2+} ion complexes on the channel walls, a small amount of the Ni^{2+} ions are reduced to Ni atoms on the bottom Au layer. At the same time, $AuCl_4^-$ ions are also reduced to Au atoms on the bottom Au layer when they reach the bottom of the nanochannel. Au and Ni atoms nucleate and grow upwards to form a AuNi alloy NW as a cable core from the atoms continuously produced at the bottom galvanic cell. The AuNi/Ni nanocables formed have slightly longer cable sheaths than cores at this stage. Meanwhile, Au and Ni atoms formed on the ring-shaped Al foil surface diffuse into and towards bottom of the nanochannels, because of their concentration gradient (Figure 3b, stage 2). At longer periods of infiltration, Au and Ni atoms coming from the top galvanic cell reach the tip of the AuNi alloy NW, and combine with the atoms on the NW tip coming from the bottom galvanic cell, resulting in a longer AuNi alloy NW. Continuous growth of the Ni nanotube also leads to a much longer cable sheath (Figure 3b, stage 3). The AuNi alloy NWs grow faster and faster due to the combination of Au and Ni atoms coming from the top galvanic cell with those formed at the bottom galvanic cell. Finally, AuNi/Ni nanocables with AuNi alloy cores almost as long as the Ni sheaths are formed (Figure 3b, stage 4). When the AAO template embedded with AuNi/Ni nanocables is immersed in a 3 M aqueous NaOH solution at room temperature, the Ni shells of the AuNi/Ni nanocables are oxidized to NiO rather than to $Ni(OH)_2$ by the reactions $2Ni + O_2 \rightarrow 2NiO$ and $Ni + H_2O \rightarrow NiO + H_2\uparrow$ after the AuNi/Ni nanocables are released from the AAO channel walls. This is because $Ni(OH)_2$ can only be formed in a high-concentration NaOH solution at high temperature.[24] The existence of $Ni(OH)_2$ in the cable shell can also be ruled out by further FTIR and Raman spectroscopic measurements. From FTIR spectrum of the final nanocables (Figure S2), it can be observed that there is no absorption peaks related to the O–H stretching vibration (3700–3100 cm^{-1}). In the meanwhile, the Raman spectrum (Figure S3) exhibits no characteristic bands of Ni $(OH)_2$ [312, 448, and 3582 cm^{-1} for β-$Ni(OH)_2$,[25] 465 and 3640 cm^{-1} for α-$Ni(OH)_2$[26]]. As the Ni shells of the AuNi/Ni nanocables are very thin (about tens of nanometers), they are easily oxidized totally to NiO in aqueous NaOH solution. Thus, nanocables of AuNi/NiO rather than AuNi/Ni/NiO are obtained in the end (Figure 3b, stage 5).

NiO NWs[27] and NiO NW/metal junctions[28] exhibit resistive switching behavior, demonstrating the feasibility for use in resistance memory devices; and NiO nano/microstructures[29,30] are good candidates for high performance electrochemical capacitors. Thus, our nanocables with NiO as cable shells might have potential in resistance memory devices and electrochemical capacitors.

Conclusions

We have developed a facile and economic approach to AuNi/NiO nanocables, by infiltrating Au-coated-Al-surrounded AAO templates with a mixed aqueous solution of $NiCl_2$ and $HAuCl_4$, and subsequently immersing them in an aqueous NaOH solution. Firstly, AuNi/Ni nanocables are formed in the nanochannels of the AAO template after the infiltration of the nanochannels with a mixed aqueous solution of $NiCl_2$ and $HAuCl_4$. The formation of the AuNi/Ni nanocables is due to the reduction of Ni^{2+} ion complexes adhering on the AAO channel walls to produce Ni shells and the redox reactions of two galvanic cells with the surrounding Al foil as anode, which lead to the formation of AuNi inner cores. Then, the Ni outer shells of the AuNi/Ni nanocables are totally oxidized to NiO during the removal of the AAO channel walls in an aqueous NaOH solution. As a result, nanocables of AuNi/NiO rather than AuNi/Ni/NiO are formed in the end. The shell thickness and the chemical composition of the resultant nanocables can be tailored by tuning the composition of the mixed solution. The approach could be extended to other metal-alloy/NiO nanocables by using mixed aqueous solutions of $NiCl_2$ and other water-soluble metal chloride salts.

Experimental Section

The Al-surrounded AAO templates (with pore diameters of 70–90 nm) used in the experiments were prepared by a two-step anodization process in oxalic acid solution.[31] The fabrication process of the AuNi/NiO nanocables is similar to that of metallic NWs in our previous work.[20] Firstly, a gold layer (100 nm) was sputtered onto one planar surface side of the Al-surrounded AAO template with two-end through pores. The outermost surface of the Al foil surrounding the AAO template was stuck by insulating adhesive tapes to make a very narrow ring-shaped part adjacent to the AAO exposed. Subsequently, the Au-coated-Al-surrounded AAO template mounted in a simple polymethyl methacrylate (PMMA) holder (Figure 3a) was infiltrated with a mixed aqueous solution (2 mL) of $NiCl_2{\cdot}6H_2O$ (4 M) and $HAuCl_4{\cdot}4H_2O$ (20 mM) with different volume ratios for 3 h at room temperature. Finally, the as-infiltrated AAO template was immersed in an aqueous NaOH solution (3 M) at room temperature and then washed repeatedly with deionized water. In the experiments, mixed aqueous solutions with three different volume ratios (1:0.67, 1:1, and 1:1.5) of $NiCl_2{\cdot}6H_2O$ (4 M) and $HAuCl_4{\cdot}4H_2O$ (20 mM) were employed. The molar concentrations of $NiCl_2$ in these three mixed solutions are calculated to be 2.4, 2, and 1.6 M, respectively.

Supporting Information (see footnote on the first page of this article): XRD, FTIR, and Raman spectra.

 © 2010 Wiley-VCH Verlag GmbH & Co. KGaA, Weinheim

Acknowledgments

We thank the National Natural Science Foundation of China (Grant Nos. 50525207 and 50972145), and the National Basic Research Program of China (Grant No. 2007CB936601) for financial support.

[1] J. H. He, Y. Y. Zhang, J. Liu, D. Moore, G. Bao, Z. L. Wang, *J. Phys. Chem. C* **2007**, *111*, 12152–12156.
[2] S.-W. Choi, J. Y. Park, S. S. Kim, *Nanotechnology* **2009**, *20*, 465603.
[3] A. Javey, S.-W. Nam, R. S. Friedman, H. Yan, C. M. Lieber, *Nano Lett.* **2007**, *7*, 773–777.
[4] Y. L. Cao, Y. B. Tang, Y. Liu, Z. T. Liu, L. B. Luo, Z. B. He, J. S. Jie, R. Vellaisamy, W. J. Zhang, C. S. Lee, S. T. Lee, *Nanotechnology* **2009**, *20*, 455702.
[5] M. Law, L. E. Greene, A. Radenovic, T. Kuykendall, J. Liphardt, P. D. Yang, *J. Phys. Chem. B* **2006**, *110*, 22652–22663.
[6] G. Chen, Z. Wang, D. Xia, *Chem. Mater.* **2008**, *20*, 6951–6956.
[7] Q. Wang, G. Wang, X. Han, X. Wang, J. G. Hou, *J. Phys. Chem. B* **2005**, *109*, 23326–23329.
[8] D. C. Yang, G. W. Meng, Q. L. Xu, X. L. Zhao, J. L. Liu, M. G. Kong, Z. Q. Chu, X. G. Zhu, L. D. Zhang, *Appl. Phys. Lett.* **2008**, *92*, 083109.
[9] G. S. Huang, Y. Xie, X. L. Wu, L. W. Yang, Y. Shi, G. G. Siu, P. K. Chu, *J. Cryst. Growth* **2006**, *289*, 295–298.
[10] Y. D. Yin, Y. Lu, Y. G. Sun, Y. N. Xia, *Nano Lett.* **2002**, *2*, 427–430.
[11] N. I. Kovtyukhova, T. E. Mallouk, T. S. Mayer, *Adv. Mater.* **2003**, *15*, 781–785.
[12] D. Ma, M. Zhang, G. Xi, J. Zhang, Y. T. Qian, *Inorg. Chem.* **2006**, *45*, 4845–4849.
[13] W. Xu, S.-H. Yu, *Small* **2009**, *5*, 460–465.
[14] Y. Bi, J. Ye, *Chem. Commun.* **2009**, 6551–6553.
[15] T. Ghoshal, S. Biswas, S. Kar, *J. Phys. Chem. C* **2008**, *112*, 20138–20142.
[16] Z.-Z. Li, J. Baca, S. H. Yun, J. Wu, *Nanotechnology* **2008**, *19*, 055606.
[17] E. López-Camacho, M. Fernández, C. Gómez-Aleixandre, *Nanotechnology* **2008**, *19*, 305602.
[18] K. Huang, Y. Zhang, Y. Long, J. Yuan, D. Han, Z. Wang, L. Niu, Z. Chen, *Chem. Eur. J.* **2006**, *12*, 5314–5319.
[19] G. Lu, C. Li, J. Shen, Z. Chen, G. Shi, *J. Phys. Chem. C* **2007**, *111*, 5926–5931.
[20] Q. L. Xu, G. W. Meng, X. B. Wu, Q. Wei, M. G. Kong, X. G. Zhu, Z. Q. Chu, *Chem. Mater.* **2009**, *21*, 2397–2402.
[21] A. J. Bard, R. Parsons, J. Jordan in *Standard Potentials in Aqueous Solution*, Marcel Dekker, New York, **1985**.
[22] S. S. Djokić, *J. EIectrochem. Soc.* **1996**, *143*, 1300–1305.
[23] C. R. Martin, M. Nishizawa, K. Jirage, M. Kang, *J. Phys. Chem. B* **2001**, *105*, 1925–1934.
[24] S. Z. Yao, Y. B. Zhu, S. E. He, L. H. Nie in *Handbook of Chemical Reactions of Elements*, Hunan Education Press, **1998**.
[25] X. M. Ni, Q. B. Zhao, Y. F. Zhang, J. M. Song, H. G. Zheng, K. Yang, *Solid State Sci.* **2006**, *8*, 1312–1317.
[26] D. N. Yang, R. M. Wang, M. S. He, J. Zhang, Z. F. Liu, *J. Phys. Chem. B* **2005**, *109*, 7654–7658.
[27] S. I. Kim, J. H. Lee, Y. W. Chang, S. S. Hwang, K.-H. Yoo, *Appl. Phys. Lett.* **2008**, *93*, 033503.
[28] K. Oka, T. Yanagida, K. Nagashima, T. Kawai, J.-S. Kim, B. H. Park, *J. Am. Chem. Soc.* **2010**, *132*, 6634–6635.
[29] J. W. Lang, L. B. Kong, W. J. Wu, Y. C. Luo, L. Kang, *Chem. Commun.* **2008**, 4213–4215.
[30] C. Z. Yuan, X. G. Zhang, L. H. Su, B. Gao, L. F. Shen, *J. Mater. Chem.* **2009**, *19*, 5772–5777.
[31] H. Masuda, M. Satoh, *Jpn. J. Appl. Phys.* **1996**, *35*, L126–L129.

Received: March 22, 2010
Published Online: August 24, 2010

 © 2010 Wiley-VCH Verlag GmbH & Co. KGaA, Weinheim